Riv. It. Paleont. Strat.	v. 95	n. 3	pp. 315-336	tav. 34-36	Novembre 1989

BACTERIAL COLONIES AND MANGANESE MICRONODULES RELATED TO FLUID ESCAPE ON THE CREST OF THE MEDITERRANEAN RIDGE

MARIA BIANCA CITA*, FULVIA S. AGHIB*, SILVIA AROSIO*, ELEONORA FOLCO*, LAMBERTO SARTO*, ELISABETTA ERBA* & AGOSTINO RIZZI**.

Key-words: Holocene, Eastern Mediterranean, Bacterial colonies, Fluid escape.

Riassunto. Un livello-guida nero olocenico spesso pochi centimetri è stato individuato in tutte le carote prelevate in due campi di diapiri recentemente scoperti sulla Dorsale Mediterranea a sud di Creta. Ricerche sulla ultrastruttura del livello-guida e sulla sua composizione mediante microsonda hanno rilevato la presenza di innumerevoli micronoduli di manganese e di colonie batteriche. La mineralizzazione e l'attività batterica ad essa collegata sone messe in rapporto con il rilascio di fluidi che accompagna la risalita diapirica di materiale sedimentario nel prisma di accrescimento e, tentativamente, con l'evento vulcanico di Santorini.

Abstract. A black, few centimeters thick Marker-bed of Holocene age is consistently recorded in all the deep-sea cores raised from two fields of mud diapirs recently discovered on the crest of the Mediterranean Ridge south of Crete. Detailed investigations on the ultrastructure of the Marker-bed accompained by microprobe analysis revealed the occurrence of Mn-rich micronodules and bacterial colonies in very high number. Their occurrence is accounted to fluid escape in the accretionary prism, related to mud diapirism and tentatively associated with an important volcanic event occurred in the arc-trench system.

Background.

Two fields of mud diapirs were recently discovered on the crestal area of the Mediterranean Ridge south of Crete, during a cruise of the Italian R/V BANNOCK (Cita, Camerlenghi et al., in press).

The Mediterranean Ridge is the most prominent physiographic feature of the Eastern Mediterranean, a real submerged mountain chain over 1500 km long, bound to the north by the Hellenic, Tolemy, Pliny and Strabo trenches, to the south by the Messina, Sirte, Herodotus abyssal plains (Fig. 1). It is widely accepted as an accretionary wedge related to the subduction of the African plate under the Aegean microplate (Le Pichon et al., 1979; Finetti, 1982; Ryan et al., 1982 inter alias). The Mediterranean Ridge is characterized by a strongly irregular, hummocky surface, the so-called "Cobblestone

*Dipartimento di Scienze della Terra dell'Università degli Studi di Milano, via Mangiagalli, 34, 20133 Milano.

**Centro Alpi C.N.R., via Mangiagalli, 34, 20133 Milano

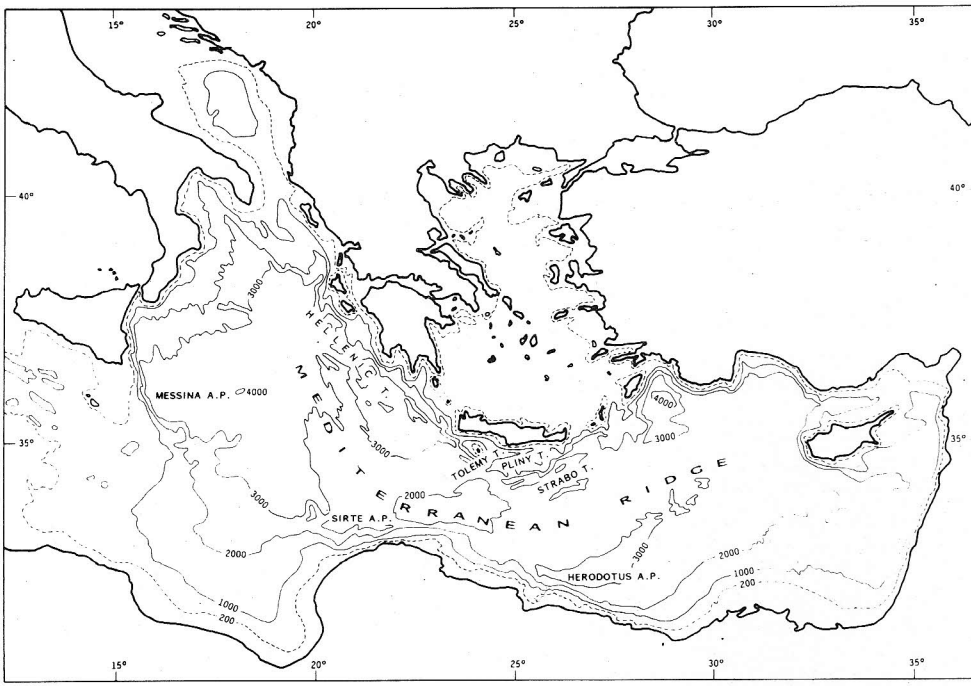

Fig. 1 - Index map.

topography" (of Emery et al., 1965) whose origin has been shown to result from a combination of tectonic deformation in a compressional regime, and submarine dissolution of Messinian evaporites (Blechschmidt et al., 1982; Camerlenghi & Cita, 1987).

A single mud diapir, that is a dome-like structure made up by a mud breccia entirely different from the surrounding lithologies, originating from the deep, was discovered ten years ago on the crestal area of the western Mediterranean Ridge west of Crete (Cita et al., 1981; Ryan et al., 1982; Cita, Bossio et al., 1984).

Two fields of mud diapirs were discovered in September, 1988 south of Crete, where compression in the Ridge is maximum, no abyssal plain exists to the south, separating the Ridge deformation front from the African margin, and continent/continent collision is occurring. Each field contains two to five discrete domes, which were mapped at the scale 1:40000 and cored during a three-days long exploration.

The domes are cone-shaped, have a diameter of approximately 2 km and an elevation of approximately 100 m. They raise above the regional landscape, characterized by the "Cobblestone topography". Their top lies consistently around 1900 m.

The cores were precisely positioned by means of a pinger: in other words, the bathymetric survey and the precise positioning of the cores allow to locate the cores with reference to the bottom configuration.

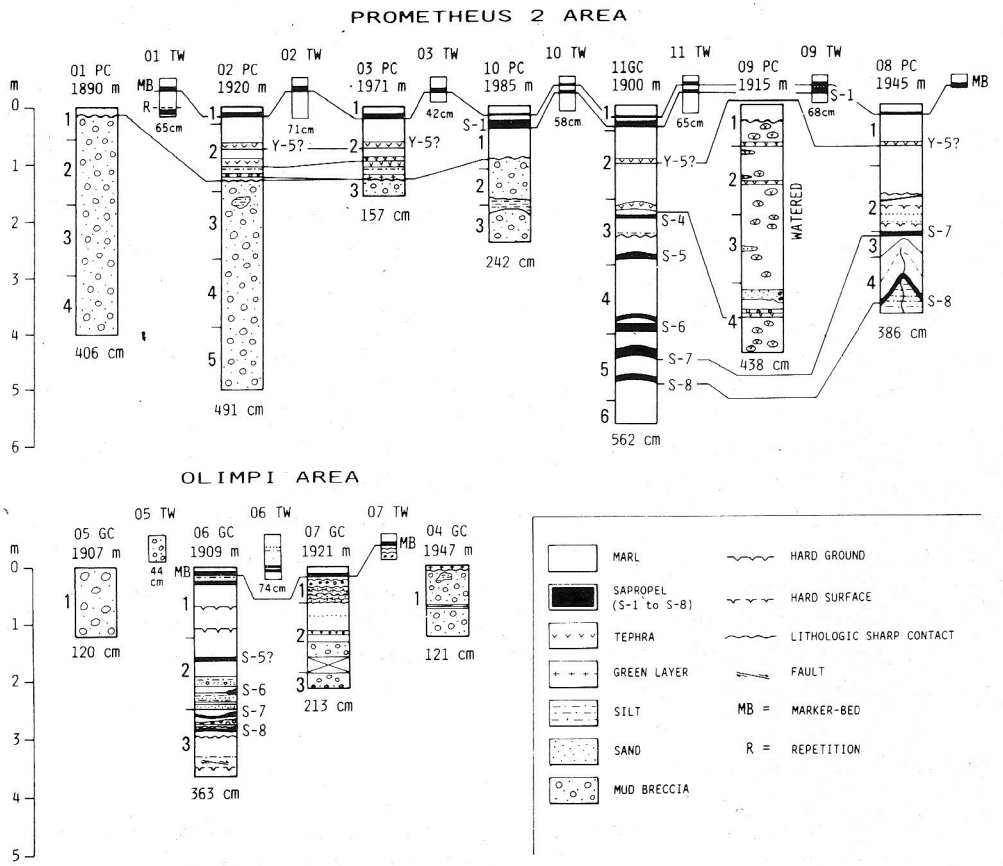

Fig. 2 - Stratigraphy of the sediment cores recovered in the two fields of mud diapirs: Prometheus 2 Area is the western field, Olimpi Area is the eastern field. PC = piston core; GC = gravity core; TW = trigger core.

The two fields of mud diapirs are some 20 km apart. Seven piston and/or gravity cores (PC and GC) were raised in the western field, named "Prometheus 2". Four gravity cores (GC) were collected in the eastern field, named "Olimpi". Cores were mounted using a trigger arm, so we have a recovery also in the trigger cores (TW) in most cases.

The domes were found to contain a mud breccia entirely different in lithologic make up and in age from the sedimentary succession of the area, which is characterized by hemipelagic marls or oozes as dominant lithology, by sapropels and tephra as minor, and isochronous lithologies (see Cita, Camerlenghi et al., in press).

A prominent, albeit thin, black Marker-bed was found in almost all the trigger, piston and gravity cores from the two diapiric fields, ten to twenty cm from the core top (=sediment/water interface). Fig. 2 illustrates the core logs: the Marker-bed is usually sandwiched between pelagic oozes, brownish in color. The only exception are cores

01 PC, 04 GC, and 05 GC, 05 TW where the mud breccia is present to the top, and no pelagic drape is recorded.

Shipboard observations showed that the Marker-bed strongly reacts with H_2O_2, and that it is metal-rich.

The Marker-bed was consistently recorded not only in the cores that contain the breccia, but also in those raised out of the domes, on plateaus.

The hypothesis that the process originating the metal-rich layers was related to the diapiric process was immediately put forward, and a shipboard detailed sampling was done on cores BAN-88 10 TW and 11 TW from the Prometheus 2 area, selected because both contain also Sapropel S-1, thus allowing a precise stratigraphic correlation.

Sapropel S-1 is an isochronous lithostratigraphic unit widespread in the Eastern Mediterranean: it correlates with the Termination I, with the end of the Flandrian transgression and with the lower part of the isotopic stage 1 (Cita et al., 1977; Vergnaud-Grazzini et al., 1977; Sutherland et al., 1984; Vismara Schilling, 1984).

Purpose of this paper is to show the results of our observations on the ultrastructure and composition of this Marker-bed, which is ubiquitous in the two newly discovered diapiric fields, but was never recorded elsewhere in the Eastern Mediterranean, where the research group of Marine Geology of the University of Milan concentrated his efforts in the last ten years, collecting and studying over 200 precisely positioned deep-sea cores.

Characters of the Marker-bed.

The cores were split shipboard, visually described, photographed (color prints) and sampled. The microscopic work carried out on the ship was based on washing residues (sediment fractions larger than 63 microns) observed with the binocular microscope, and on smear slides observed at the polarizing microscope. Colors were identified with reference to the Munsell color chart.

A shorebases, thorough comparative study of the Marker-bed was carried out on the entire data set (12 cores from the Prometheus 2 area; 3 cores from the Olimpi area) based on shipboard description and color prints. The following characters were analyzed: color, thickness, lower boundary, upper boundary. They are summarized in Tab. 1, which also provides information on the coordinates, water depth, and setting of each core.

A few comments follow:

The lower boundary of the Marker-bed is mostly sharp and distinct, unlike the upper boundary, which is usually gradational. The boundaries are diagonal 11 times out of 15. When the boundary (ies) is not sharp, thickness was measured excluding the fading part.

Thickness of the Marker-bed ranges from 1.5 to 4 cm. The lesser thickness is recorded on dome tops (cores BAN-88 01 TW) and on a plateau out of the diapiric structures (cores BAN-88 09 TW, 11 GC). Maximum thickness is recorded on the flanks of

CORE	LATITUDE	LONGITUDE	DEPTH	SETTING	THICKNESS	COLOR	LOWER BOUNDARY	UPPER BOUNDARY
01 TW	33° 49. 95' N	24° 25. 96' E	1890 m	dome top	1,5 cm	5YR 2.5/1 black	distinct, diagonal	fading, diadonal
02 PC	33° 50. 10' N	24° 25. 10' E	1920 m	W flank of dome	4 cm	10YR 2/1 black	fading, diagonal	distinct, diagonal
02 TW	33° 50. 10' N	24° 25. 10' E	1920 m	W flank of dome	3 cm	10YR 2/1 black	distinct, diagonal	fading,diagonal
03 PC	33° 49. 75' N	24° 25. 63' E	1971 m	S flank of dome	2 cm	5Y 2.5/1 black	fading, diagonal	fading, diagonal
03 TW	33° 49. 75' N	24° 25. 63' E	1971 m	S flank of dome	3 cm	5Y 2.5/1 black	distinct, horizontal	distinct, diagonal
06 GC	33° 45. 10' N	24° 43. 48' E	1909 m	dome top	2 cm	10YR 3/1 very dark gray	fading, horizontal	fading, horizontal
07 GC	33° 43. 87' N	24° 43. 47' E	1921 m	SW flank of upper dome	2 cm	5Y 3/1 very dark gray	fading, diagonal	fading, diagonal
07 TW	33° 43. 87' N	24° 43. 47' E	1921 m	SW flank of upper dome	4 cm	5Y 3/1 very dark gray	fading, diagonal	fading, diagonal
08 PC	33° 48. 95' N	24° 26. 02' E	1945 m	slope near plateau	2 cm	7.5YR 2/0 black	distinct, diagonal	fading, diagonal
08 TW	33° 48. 95' N	24° 26. 02' E	1945 m	slope near plateau	3 cm	7.5YR 2/0 black	distinct, diagonal	fading, diagonal
09 TW	33° 48. 95' N	24° 26. 02' E	1915 m	SW plateau	1,5 cm	7.5YR 2/0 black	distinct, horizontal	fading, horizontal
10 PC	33° 49. 63' N	24° 26' E	1985 m	depression, SE of dome	3 cm	10YR 2/1 black	distinct, diagonal	fading, diagonal
10 TW	33° 49. 63' N	24° 26' E	1985 m	depression, SE of dome	4 cm	5YR 2.5/1 black	distinct, diagonal	distinct, diagonal
11 GC	33° 49. 10' N	24° 24. 71' E	1900 m	SW plateau	1,5 cm	5YR 2.5/1 black	distinct, diagonal	fading, diagonal
11 TW	33° 49. 10' N	24° 24. 71' E	1900 m	SW plateau	2 cm	7.5YR 2/0 black	distinct, horizontal	fading, horizontal

Tab. 1 - Visual characters of the Marker-bed in the cores investigated, and their location.

the domes. A transect of cores taken on Prometheus 2 Dome shows that thickness of the Marker-bed increases downslope (Tab. 2).

Burrowing is never observed in the Marker-bed, whereas faint laminations are occasionally recorded.

Two samples of the normal sediment were analyzed by X Ray diffractometry at the Geochemical Laboratory of AGIP s.p.a. (S. Donato Milanese) to check the major components and the clay mineral composition.

CORE	DEPTH	THICKNESS
01 TW	1890 m	1,5 cm
03 PC	1971 m	2 cm
03 TW	1971 m	3 cm
10 PC	1985 m	3 cm
10 TW	1985 m	4 cm

Tab. 2 - Variations in thickness of the Marker-bed observed in Prometheus 2 Dome.

Sample BAN-88 01 TW, sampled at 30 cm from the core top, beneath the Marker-bed does not contain any clay. It consists of 89% calcite, 9% qz and 2% K feldspar. The occurrence of pyrite and siderite was noticed.

Sample BAN-88 01 PC, sampled at 52 cm from the core top beneath Sapropel S-1 consists of 20% clay, 61% calcite (38% of which is Magnesian calcite, 23% calcite), 19% qz. The clay minerals identified are 18% smectite, 29% illite, 35% kaolinite, 18% chlorite.

Study of cores BAN-88 10 TW and 11 TW.

Two trigger cores were sampled at closely spaced intervals (one observation point every approximately 2000 y) in order to check the changes in the various sedimentary parameters. Fig. 3 shows the two halves of Core 10 TW, containing two prominent dark layers: the metalliferous Marker-bed and, some 8 cm lower in the section, Sapropel S-1; the latter is bioturbated and contains numerous pteropod shells, unlike the former.

The sediment samples of both cores were split: one gram was used for calcimetry, using a Dieterich-Freeling calcimeter; the remaining part was weighted, washed, sieved through a 63 microns mesh, and the residues were weighted again. The percentage of the sediment fraction greater than 63 microns was then calculated.

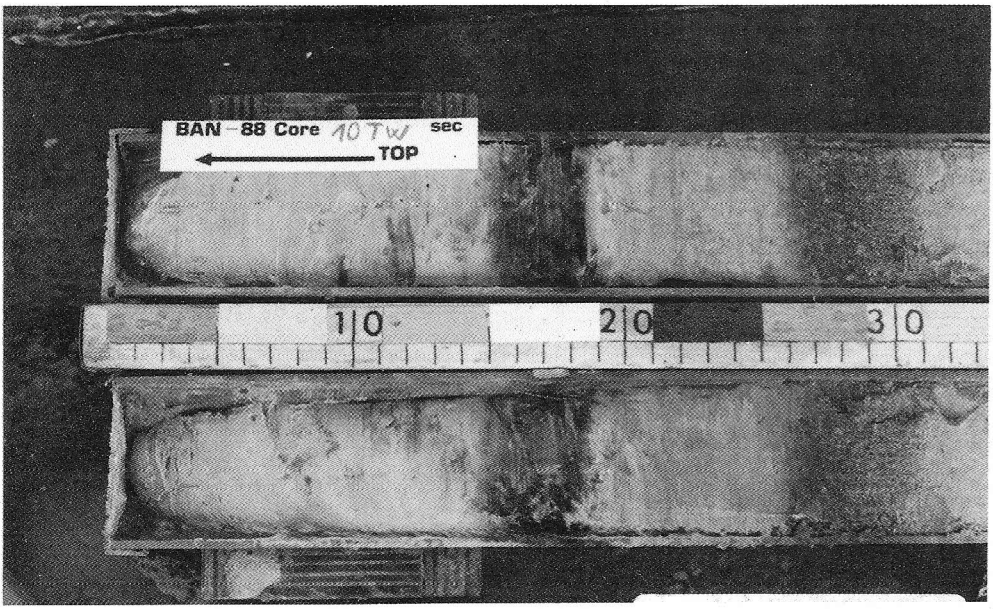

Fig. 3 - Photo of the split upper part of Core BAN-88 10 TW showing two prominent dark layers: the metalliferous Marker-bed and, 8 cm underneath, Sapropel S-1. The latter, unlike the former, is bioturbated and has gradational boundaries.

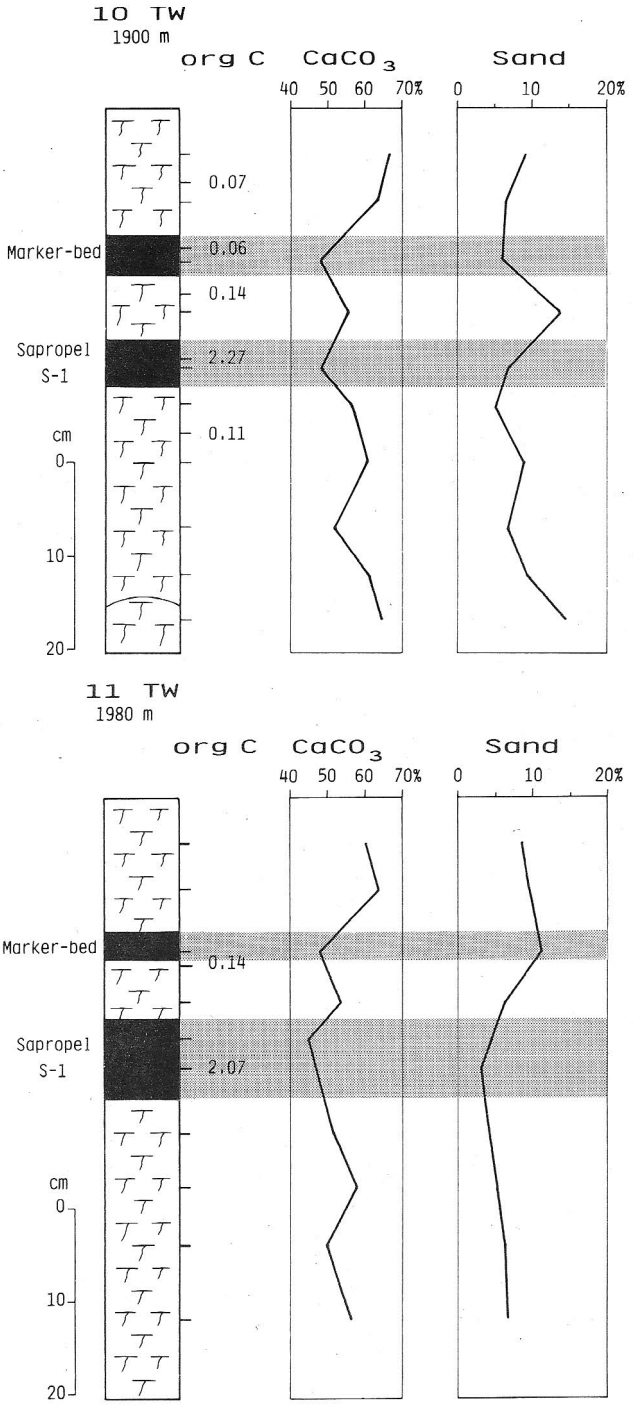

- Lithologic log, organic carbon percentages, calcium carbonate content curves and percentages of the sand-size fraction measured in cores BAN-88 10 TW and 11 TW.

The variations observed in the carbonate content and in the sand-size sediment fraction are shown in Fig. 4.

Negative peaks of the carbonate content are recorded in both cores in the black Marker-bed as well as in Sapropel S-1. The sand-size fraction ranges from a few percent to over 14%. No definite trend is recorded.

Five samples from Core 10 TW, including the Marker-bed and Sapropel S-1 were analyzed in their content in organic carbon, using a LECO auto-analyzer (measurements made at Laboratorio Geochimico of AGIP s.p.a., S. Donato Milanese).

The values obtained are also shown in Fig. 4. All the values are very low, including the Marker-bed. The only exception is Sapropel S-1 which contains 2.27% org C and consequently falls into the category of true sapropels according to Kidd et al. (1978).

Analyses of the organic carbon content were also applied to the Marker-bed and to the Sapropel S-1 of Core BAN-88 11 TW. Also in this case, the value obtained for the Marker-bed is very low, whereas Sapropel S-1 contains a fairly high percentage of org C (2.07%).

	TW 11 16,5 cm Marker-bed ground mass	TW 11 16,5 cm Marker-bed micronodule	TW 11 26 cm Sapropel S-1 ground mass	TW 11 26 cm Sapropel S-1 framboid	
Na	8.01	7.56	2.94	2.47	%
Mg	5.35	7.26	2.90	1.70	%
Al	1.81	2.28	4.81	1.38	%
Si	3.03	2.59	11.85	1.98	%
P	0.15	0.08	0.41	0.37	%
S	5.92	7.22	1.19	45.22	%
Cl	4.56	2.35	4.96	2.02	%
K	1.24	1.30	1.02	0.28	%
Ca	8.55	7.27	24.76	4.66	%
Mn	26.75	40.26	0.12	0.50	%
Fe	0.86	1.14	3.33	42.03	%
Ti	0	0	0.30	0.04	%
MATRIX	33.77	20.69	41.42	2.67	%
TOTAL	100.00	100.00	100.00	100.00	%

Tab. 3 - Quantitative analytical composition, by X-ray diffractometry, of the Marker-bed and Sapropel S-1 in Core BAN-88 11 TW.

Ultrastructure and composition of the Marker-bed versus Sapropel S-1.

In order to ascertain the nature of the Marker-bed and to substantiate the differences versus Sapropel S-1, it was decided to observe the bulk sediment at the Scanning Electron Microscope (SEM). The sediment was gold-coated. At increasing magnifications (see Pl. 34, fig. 1 a-c) the images show micronodules covered by a network of coalescent structures that are interpreted as bacterial colonies.

Low magnification SEM investigations detected a matrix consisting of nannofossils, minor quantities of foraminifers and of nodular structures (Pl. 34, fig. 1 and 2).

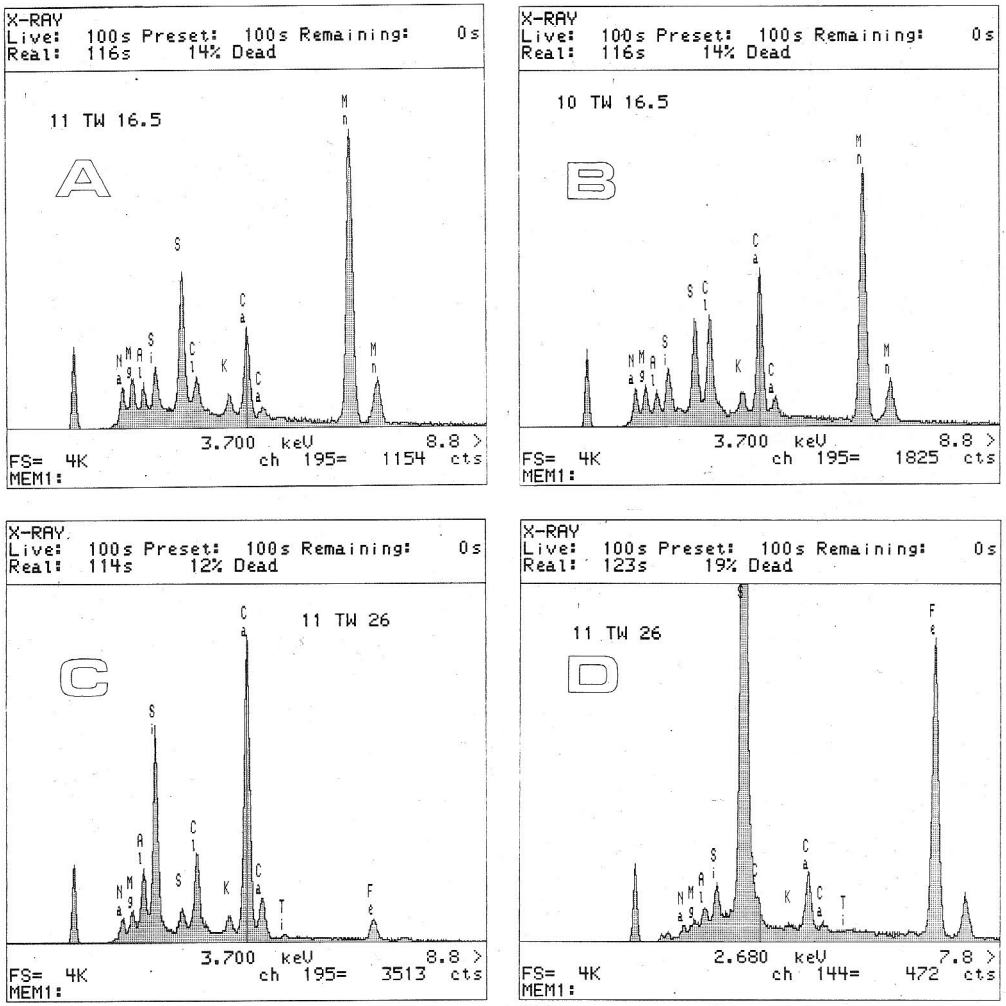

Fig. 5 - Diffractograms of the Marker-bed (A,B) and of Sapropel S-1 (C,D). For additional comments, see text.

Nodular structures range in diameter from a few microns to 10 microns (micronodules).

Chemical analyses, performed with EDAX microprobe executed on the individual nodules revealed an extraordinary concentration of Mn, up to 40.26% (see Tab. 3).

Using high magnification (10000x-120000x) on gold-covered samples, it was possible to observe in detail the structure of the manganese micronodules. They appear to be built out of bacterial colonies; spherical shapes could be cocchi (Pl. 35, fig. 4), while the cylindrical ones are interpreted as bacilli (Pl. 35, fig. 3).

Yet, considering the result of chemical analyses, where Ca and Mg are shown to exist in greater quantity than P and K, the presence of bacterial spores can also be inferred (Pl. 34, fig. 2c); it is important to remember, anyway, that such bacterial spores and bacteria are identical, except for the chemical composition of the cell wall and overall dimension. These differences allow the spores to survive in harsher environments: it is a biological adaptation with survival value.

Organic carbon in the sample is practically non-existent (Fig. 4): this can be explained with the presence of bacteria which oxidate the manganous ion and use organic carbon in their metabolism (Alexander, 1977).

Microprobe analyses were carried out both on gold-coated samples and, to avoid disturbances, also on graphite-coated samples. Overall, 22 EDAX diffractograms were performed.

A few diffractograms are shown in Fig. 5.

Diffr. A is from the Marker-bed sampled in Core BAN-88 11 TW (16.5 cm from core top): a distinct Mn peak is shown in the ground-mass. Diffr. B is from the Marker-bed sampled in Core BAN-88 10 TW (16.5 cm from the core top): it shows a similar distinct Mn peak. Diffr. C is from the ground-mass of Sapropel S-1 sampled at 26 cm from the top in Core BAN-88 11 TW: it shows no Mn, but peaks in Ca and Si which are accounted to biogenic calcitic components and to clay minerals respectively. Diffr. D is from a pyrite framboid in Sapropel S-1 (same sample as for C) and shows a very strong peak in S, followed by a peak in Fe.

Quantitative X Ray analyses were also carried out with EDAX on 12 samples overall, including the ground-mass of the Marker-bed and of Sapropel S-1, micronodules (pirolousite or manganite) and pyrite framboids. Tab. 3 shows the results obtained on four selected samples.

The ultrastructure of Sapropel S-1 sampled in Core BAN-88 11 TW was investigated using the same procedures. Pl. 35, fig. 1a-c, show a selection of images: framboidal pyrite, numerous coccoliths, clay laminae are visible, but *no bacteria.*

Investigations on the ultrastructure were also carried out on a few samples of the Marker-bed from Cores BAN-88 01 TW and 09 TW. These samples, unlike those discussed so far, were shipboard treated using hydrogen peroxyde. We wanted to test eventual differences in bacterial abundance, since the strong reaction recorded should have oxydized all the organic matter. Pl. 36 documents our findings. The washing residue

which was the richest in metallic concretions (Pl. 36, fig. 1a-c) contains a few bacteria, but the washing residue that contains micronodules and biogenic components is as rich in bacterial colonies as the unprocessed samples (compare fig. 2c of Pl. 36 with fig. 1c of Pl. 34).

Discussion.

The Mn-rich Marker-bed may be compared with similar findings in the Eastern Mediterranean and in the open ocean.

Mn- and Fe-rich layers have been recently documented in hemipelagic sediments from the Eastern Mediterranean (Pruysers et al., 1989). Particularly a discrete Mn peak occurs a few centimeters above Sapropel S-1, within brown oozes. It has no macroscopic evidence and in fact it was identified by means of geochemical analyses. These metal-rich layers do not show any evidence of bacterial activity. Mn- and Fe-rich spikes are related to early diagenetic processes such as post-depositional remobilization and reprecipitation of Mn-oxides and Fe- oxihydroxides. At the redox front, when stady state conditions are established, Mn- and Fe-rich layers form.

Mn-Fe coatings were reported from the Mediterranean also by Allouc (1988). They are very thin lithified incrustations with botryoidal surface and characterized by microborings. Similar Mn-crusts and nodules recovered from the Central Pacific Ocean were studied in detail by Janin (1987). They seem to result from the progressive mineralization of a stromatolitic framework. Both these metal-rich deposits are related to extremely low accumulation rates and to early diagenetic processes leading to hardground formation. Also in this case although bacterial activity is likely to have interfered, no direct evidence have been collected so far.

The Marker-bed documents a strong bacterial activity. For this reason, it may be compared to bacterial-related sediments recently discovered in deep anoxic basins of the Eastern Mediterranean (Erba et al., 1987; Erba & Parisi, 1987; Erba, 1989; Rodondi & Andreis, 1989). In this case sulfate-reducing bacteria grow at the normal sea water/brine interface located at approximately 3200 m depth. They produce peculiar gelatinous pellicles consisting of amorphous organic matter entrapping biogenic and inorganic debris. Discrete layers of bacterial pellicles have been observed in several cores collected from the anoxic basins and interlocked within gypsum crystals dredged from the steep slopes of the Bannock Basin. Such pellicles are recorded at different depths within cores, thus testifying a repetitive process. Unlike the Marker-bed, they do not show any metal-enrichment or micronodular structures.

In conclusion, the characters of the Marker-bed are unique and none of the processes discussed above can explain its origin.

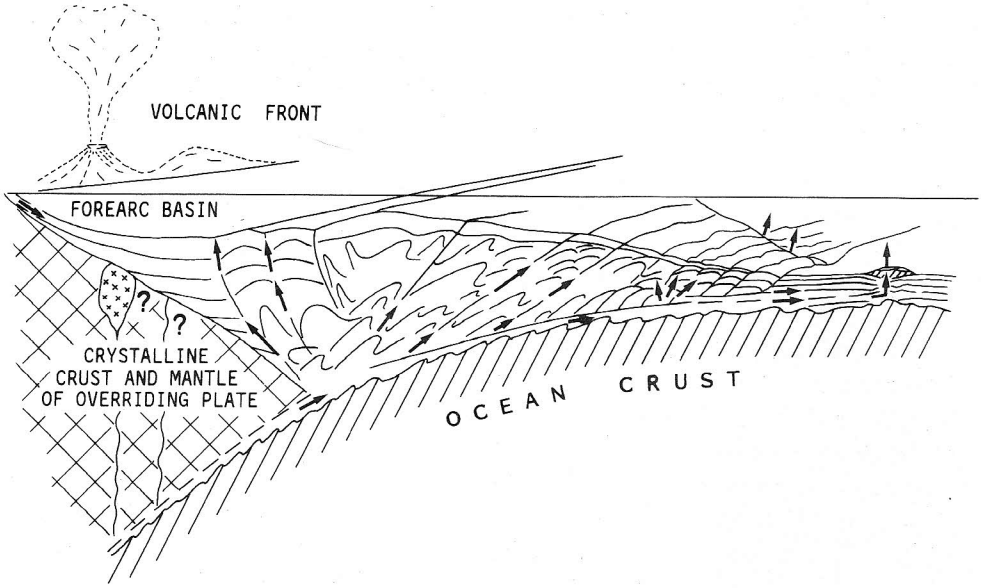

Fig. 6 - Scheme of fluid circulation in an accretionary prism (after Cosod 2, 1987, modified).

Hypothesis on the origin of the Marker-bed.

A corollary of the accretionary prisms model is fluid escape. Fluids, that is mineralized water, methane, move along the subduction plane, along décollement surfaces, along thrust planes and reach the ocean floor in front of the wedge and on the wedge itself, in different situations (Fig. 6).

The process of mud diapirism is unconceivable without fluid motion. The mud breccia that we cored repeatedly in the two diapiric fields has to be accompained by fluids (liquid and/or gaseous) that we were unable to sample so far because no suitable tool was available on the ship.

Additional coring and sampling is planned in order to fill this gap in our knowledge.

However, the discovery of the metalliferous Marker-bed with its countless bacterial colonies is a tangible proof of fluid escape. The manganobacteria would develop from the metal-rich fluids of deep origin when they reach the sea floor, and are mixed with normal sea-water.

The strong differences that we recorded (a) versus manganiferous laminae related to the diagenetic migration of the redox front and (b) versus bacterial laminae forming at the brine/normal sea-water interface, as discussed in the previous chapter, support the assumption that the process under examination is indeed related to fluid escape unlike the formers, also documented in the Eastern Mediterranean and accounted to entirely different processes.

	DISTANCE FROM:	
	CORE TOP/TOP MARKER BED	BASE MARKER BED/TOP S-1
01 TW	about 19 cm	-----
02 TW	about 19 cm	-----
02 PC	about 12 cm	-----
03 TW	about 18 cm	-----
03 PC	about 14 cm	-----
06 GC	about 8 cm	-----
07 TW	about 20 cm	-----
07 GC	about 13 cm	-----
08 TW	about 19 cm	-----
08 PC	about 15 cm	-----
09 TW	about 21 cm	5 CM
10 TW	15 cm	8 CM
10 PC	about 14 cm	8 CM
11 TW	about 15 cm	5,5 CM
11 GC	about 18 cm	4,5 CM

Tab. 4 - Distance of the Marker-bed relative to core top, and to the top of Sapropel S-1, in the cores investigated.

If the origin of the micronodules and related bacterial colonies appear to us quite plausible, a puzzling problem is: why a Marker-bed? Why a discrete, individual layer of fairly uniform thickness and exceptionally constant characters? Why is the layer recorded with identical characters both on the mud volcanoes and on nearby non diapiric structures, as shown by the comparison between cores BAN-88 10 TW, located on a depression at the foot of the dome, overlying the mud breccia, and BAN-88 11 TW, located on a nearby plateau, where no breccia exists?

The diapiric extrusion is a discontinuous phenomenon, as discussed elsewhere (Cita, Bossio et al., 1984; Cita, Camerlenghi et al., in press) and seems to be realized by means of multiple injections.

The lithostratigraphy of our cores (Fig. 2) clearly shows that the contact between the mud breccia - sedimentary expression of the diapiric extrusion - and the pelagic drape is diachronous, and that the age of the contact is younger near the top of the structures, where the pelagic drape may be missing altogether as in core BAN-88 01 PC, 04 GC, 05 GC, 05 TW.

Consequently, one would expect a series of metal-rich layers, each related to an individual injection, or a discontinuous interval containing variable amounts of micronodules, instead of a single Marker-bed, if diapirism was indeed the only "forcing function".

In order to narrow the boundary-conditions by evaluating the age of the "Marker-bed event" we compared its position versus the top of the core (=time zero) and, where present, versus the top of Sapropel S-1, with an estimated age of 8000 y BP. Tab. 4 summarizes the data. Taking into account that the topmost part of the sediment core is usually soupier and most watery than the lower one, age of the "Marker-bed event" should not be older than 4000 y BP.

In just that time interval a catastrophic event shocked the Eastern Mediterranean, that is the Bronze-age eruption of Santorini, followed by the collapse of the caldera and related tsunami.

A gigantic turbidite recorded in several dozens deep-sea cores and displaying different characters in different settings (Kastens & Cita, 1981; Cita et al., 1982; Cita et al., 1984; Hieke, 1984; Cita & Camerlenghi, 1985; Parisi et al., 1987; Erba et al., 1987) is interpreted as tsunami-derived.

But fluids accompanying the diapiric extrusion and originating the metal-rich bacterial colonies layer derive from the deep, and therefore should be independent from surficial phenomena such as compression and decompression created by the passage of the tsunami wave.

Looking for a second "forcing function", we found the only plausible mechanism in the Bronze-age Santorini event itself.

The coordinates of the Santorini caldera are 36° 40' N, 25° 20' E, that is some 300 km to the NNE of our diapiric fields, both lying along the same transect across the arc-trench system, perpendicular to the ridge axis and to the African margin.

With reference to Fig. 6, Santorini belongs to the volcanic front and the Mediterranean Ridge is the accretionary prism in front of the forearc basin.

Is that possible that our metal-rich layer documents the sudden release of fluids in the system accompanying the emplacement of magma in the magma chamber? The sharp, clear-cut nature of the basal contact of the Marker-bed agrees well with this hypothesis, which is also supported by the volcanogenic nature of bacterial growth. We plan to investigate the trace elements from the Marker-bed in order to eventually discriminate between a hydrothermal versus a hydrogenous origin.

According to this tentative hypothesis that we entertain, the fluids path should follow the subduction plane beneath Crete and beneath the Pliny trench.

Acknowledgments.

We wish to thank prof. C. Longo for valuable discussions on living bacteria, and Jane Whelan for discussions on bacterial activity in marine sediments. Angelo Camerlenghi and Floyd McCoy are greatly acknowledged for suggestions and discussions on various aspects related to mud diapirism.

The analytical data concerning the content in organic carbon and X ray diffractometry were generously provided by AGIP s.p.a. (Geochemical Laboratory).

We also thank Prof. Carla Rossi Ronchetti for the critical review of the manuscript.

Sincere thanks are extended to the crew and the officers of R/V BANNOCK.

Funding was provided by CNR through grant 88.01650.05 to MBC.

REFERENCES

Alexander M. (1977) - Introduction to Soil Microbiology. Cornell Univ., II Edit., pp. 1-467, John Wiley & Sons.

Allouc J. (1988) - Minéralisations ferromanganésifères associées aux sédimentations condensées des pentes continentales de Méditerranée. *Mem. Soc. Geol. It.*, v. 36, pp. 201-216, 1 pl., 4 fig., 2 tab., Roma.

Blechschmidt G., Cita M. B., Mazzei R. & Salvatorini G. (1982) - Stratigraphy of the Western Mediterranean and Southern Calabrian ridges, Eastern Mediterranean. *Mar. Micropal.*, v. 7, pp. 101- 134, 4 pl., 10 fig., 1 tab., Amsterdam.

Camerlenghi A. & Cita M. B. (1987) - Setting and tectonic evolution of some Eastern Mediterranean deep-sea basins. *Mar. Geol.*, v. 75, pp. 31-56, 19 fig., 1 tab., Amsterdam.

Cita M. B., Bossio A., Colombo A., Gnaccolini M., Salvatorini G., Kastens K. A., McCoy F. W., Broglia C., Camerlenghi A., Catrullo D., Croce M., Giambastiani M., Malinverno A. & Parisi E. (1984) - Stratigraphy and neotectonics in the Eastern Mediterranean Ridge. Cobblestone area-3, re-visited. *Mem. Soc. Geol. It.* v. 24 (1982), pp. 443-458, 8 fig., 3 tab., Roma.

Cita M. B. & Camerlenghi A. (1985) - Effetti dell'Eruzione Minoica di Santorino sulla sedimentazione abissale olocenica nel Mediterraneo Orientale. *Rend. Acc. Naz. Lincei*, v. 77, pp. 177-187, 5 fig., 3 tab., Roma.

Cita M. B., Camerlenghi A., Erba E., McCoy F. W., Castradori D., Cazzani A., Guasti G., Giambastiani M., Lucchi R., Nolli V., Pezzi G., Redaelli M., Rizzi E., Torricelli S. & Violanti D. - Discovery of mud diapirism in the Mediterranean Ridge. A preliminary report. *Boll. Soc. Geol. It.*, 4 fig., 1 tab., Roma, in press.

Cita M. B., Camerlenghi A., Kastens K. A. & McCoy F. W. (1984) - New findings of Bronze Age Homogenites in the Jonian Sea: Geodynamic Implications for the Mediterranean. *Mar. Geol.*, v. 55, pp. 47-62, Amsterdam.

Cita M. B., Maccagni A. & Pirovano G. (1982) - Tsunami as triggering mechanism of Homogenite recorded in areas of the Eastern Mediterranean characterized by the Cobblestone topography. In Saxon S. & Nieuwenhius J. K. (Eds.) - Marine Slides and other Mass Movements, pp. 233-260, 14 fig., 4 tab., Plenum Publishing Corp., New York.

Cita M. B., Ryan W. F. B. & Paggi L. (1981) - Prometheus mud-breccia: An example of shale diapirism in the Western Mediterranean Ridge. *Ann. Géol. Pays Hellén.*, v. 30, pp. 543- 570, 10 fig., 6 tab., Athens.

Cita M. B., Vergnaud-Grazzini C., Robert C., Chamley H., Ciaranfi N. & D'Onofrio S. (1977) - Paleoclimatic record of a long deep-sea core from the Eastern Mediterranean. *Quat. Res.*, v.

8, pp. 205-235, 11 fig., 4 tab., Seattle.

Cocuzza G. (1982) - Corso di Microbiologia. II Ediz. a cura di G. Nicoletti & A. Castro. Vol. di 846 pp., Leonardo Ciurca Edit., Catania.

COSOD II (1987) - Fluid circulation in the crust and global geochemical budget. *Report Second Confer. Scient. Drilling*, Strasbourg (France) 6-8 July 1987, JOIDES-ESF, pp. 67-86, 5 fig., 2 tab., Strasbourg.

Emery K. O., Heezen B. C. & Allen T. D. (1965) - Bathymetry of the Eastern Mediterranean Sea. *Deep Sea Res.*, v. 13, pp. 173-192, Oxford.

Erba E. (1989) - New findings of gelatinous pellicles from the anoxic Bannock and Tyro basins. In Cita M. B., Camerlenghi A. & Corselli C. (Eds.) - Anoxic Basins of the Eastern Mediterranean - Results of the Third Conference, Bergamo Dec. 14-16 1988, *Ricerca Sc. Educ. Perm.*, Suppl. n. 72, pp. 45-46, Milano.

Erba E. & Parisi E. (1987) - Lamine gelatinose ritrovate in un bacino anossico del Mediterraneo Orientale. *Rend. Acc. Naz. Lincei*, v. 80, pp. 299-306, 1 pl., 3 fig., Roma.

Erba E., Parisi E. & Cita M. B. (1987) - Stratigraphy and sedimentation in the western Strabo Trench, Eastern Mediterranean. *Mar. Geol.*, v. 75, pp. 57-75, 10 fig., 5 tab., Amsterdam.

Erba E., Rodondi G., Parisi E., Ten Haven H. L., Nip M. & De Leeuw J. W. (1987) - Gelatinous pellicles in deep anoxic hypersaline basins from the Eastern Mediterranean. *Mar. Geol.*, v. 75, pp. 165-183, 11 fig., 4 tab., Amsterdam.

Finetti I. (1982) - Structure, stratigraphy and evolution of Central Mediterranean. *Boll. Geof. Teor. Appl.*, v. 96, pp. 247-315, 4 pl., 34 fig., Trieste.

Hieke W. (1984) - A thick Holocene Homogenite from the Jonian Abyssal Plain. *Mar. Geol.*, v. 55, pp. 63-78, 5 fig., 1 tab., Amsterdam.

Janin M. C. (1987) - Micropaléontologie de concrétions polymétalliques du Pacifique Central: Zone Clarion-Clipperton, Chaine Centre-Pacifique, Iles de la Ligne et Archipel des Touamoutou (Eocène-Actuel). *Mém. Soc. Géol. France*, Mem. 152, 315 pp., 64 pl., 60 fig., 17 tab., Paris.

Kastens K. A. & Cita M. B. (1981) - Tsunami-induced sediment transport in the Abyssal Mediterranean Sea. *Geol. Soc. Amer. Bull.*, v. 92, pp. 845-857, 10 fig., 1 tab., Boulder.

Kidd R. B., Cita M. B. & Ryan W. B. F. (1978) - Stratigraphy of Eastern Mediterranean sequences recovered during the DSDP Leg 42A and their paleoenvironmental significance. In Hsu K. J., Montadert L. et al. - *Init. Repts. DSDP*, v. 42A, pp. 421-443, 13 fig., 4 tab., Washington D. C.

Le Pichon X., Angelier J., Aubouin J., Lyberis N., Monti S., Renard V., Got H., Mart Y., Mascle J., Mattheus D., Mitropulos D., Tsoflias P. & Chronis G. (1979) - From subduction to transform motion: A seabeam survey of the Hellenic Trench system. *Earth Planet. Sci. Lett.*, v. 4, pp. 441-450, 6 fig., Amsterdam.

Parisi E., Erba E. & Cita M. B. (1987) - Stratigraphy and sedimentation in the anoxic Bannock Basin (Eastern Mediterranean). *Mar. Geol.*, v. 75, pp. 93-117, 12 fig., 6 tab., Amsterdam.

Pruysers P. A., De Lange G. J. & Middleburg J. J. (1989) - The formation of metal-rich layers at the oxic-anoxic boundary near sapropels in sediments from the Eastern Mediterranean. In Cita M. B., Camerlenghi A. & Corselli C. (Eds.) - Anoxic Basins of the Eastern Mediterranean - Results of the Third Conference, Bergamo Dec. 14-16 1988, *Ricerca Sc. Educ. Perm.*, Suppl. n. 72, pp. 58-59, 1 fig., Milano.

Rodondi G. & Andreis C. (1989) - Biological approach to the gelatinous pellicles from a deep anoxic basin in the Eastern Mediterranean. In Cita M. B., Camerlenghi A. & Corselli C. (Eds.) - Anoxic Basins of the Eastern Mediterranean - Results of the Third Conference, Ber-

gamo Dec. 14-16 1988, *Ricerca Sc. Educ. Perm.* Suppl. n. 72, pp. 47-49, 1 pl., 1 fig., Milano.

Ryan W. B. F., Kastens K. A. and Cita M. B. (1982) - Geological evidence concerning compressional tectonics in the Eastern Mediterranean. *Tectonophysics,* v. 86, pp. 213-242, 9 fig., Amsterdam.

Sutherland H. E., Calvert S. E. & Morris R. J. (1984) - Geochemical studies of the recent sapropel and associated sediments from the Hellenic Outer Ridge, Eastern Mediterranean Sea, 1: Mineralogical and chemical composition. *Mar. Geol.*, v. 56, pp. 93-118, 6 fig., 3 tab., Amsterdam.

Vergnaud-Grazzini C., Ryan W. B. F. & Cita M. B. (1977) - Stable isotopic fractionation, climate changes and episodic stagnation in the Eastern Mediterranean during the Late Quaternary. *Mar. Micropal.*, v. 2, pp. 353-370, 7 fig., 2 tab., Amsterdam.

Vismara Schilling A. (1984) - Holocene stagnation event in the Eastern Mediterranean. Evidence from deep-sea benthic Foraminifera in the Calabrian and western Mediterranean Ridges. *Benthos'83. 2nd Int. Symp. Benthic Foraminifera (Pau, April 1983)*, pp. 585-596, 2 pl., 4 fig., 3 tab., Pau.

PLATE 34

Fig. 1 a-c - Ultrastructure of the ground-mass of the Marker bed sampled at 16.5 cm from the core top in Core BAN-88 10 TW. Untreated sample, gold-coated. a) The picture shows abundant micronodules and several coccoliths of *Emiliania huxleyi;* 1600x. b) At greater magnification the micronodules appear to be formed by bacterial growth; 4400x. c) Detail of fig. 1b, showing interlocking bacterial chains; 19000x.

Fig. 2 a-c - Ultrastructure of the ground-mass of the Marker-bed sampled at 16.5 cm from the core top in Core BAN-88 10 TW. Untreated sample, gold-coated. Increasing magnifications (a, 3000x; b, 6100x; c, 22000x). Coccoliths of *Emiliania huxleyi* (small arrows) are present in the cavities separating the micronodules and are trapped within the micronodules. Bacteria (large arrows) are less numerous in this portion of the Marker-bed than in the portion shown in fig. 1 a-c. A probable spore is encircled.

PLATE 35

Fig. 1 a-c - Ultrastructure of the ground-mass of Sapropel S-1 sampled at 29 cm from the core top in Core BAN-88 11 TW. a) (2400x) and b) (2200x) show the ground-mass, which consists of alternating laminae rich in nannofossils (E = *Emiliania huxleyi*, U = *Umbilicosphaera sibogae*, H = *Helicosphaera carteri*, S = *Syracosphaera pulchra*, S1 = *Scyphosphaera* sp., and T = *Thoracosphaera* sp.), and in clay minerals. Pyrite framboids are also shown. c) Detail of framboidal pyrite; 10700x. The diffractogram of Fig. 5 shows strong peaks of S and Fe related to pyrite framboids.

Fig. 2 - Detail of a bacterial chain from the Marker-bed sampled in Core BAN-88 11 TW (16.5 cm from the core top); 42000x.

Fig. 3 - Probable filamentous bacterial colony. Marker-bed sampled in Core BAN-88 11 TW (16.5 cm from the core top); 59000x.

Fig. 4 - Detail of inorganic laminated matrix (clay?). Probable bacteria are encircled; 16000x. Marker-bed sampled in Core BAN-88 10 TW (16.5 cm from the core top).

PLATE 36

Fig. 1 a-c - Ultrastructure of the ground-mass of the Marker-bed sampled at 20 cm from the core top in Core BAN-88 01 TW. The sediment was soaked in H_2O_2, washed and sieved through a 63 microns mesh. The residue consists of metallic aggregates (probably pirolousite or manganite) in great abundance. The residue was gold-coated and observed at the SEM. a) Numberless micronodules; 490x. b) Clay laminae and coccoliths of *Emiliania huxleyi* surrounding the micronodules; 2100x. c) Detail of 1b: arrows indicate the few bacteria left after the strong oxydizing reaction. E = *Emiliania huxleyi*, F = *Flabellisphaera profunda*; 10900x.

Fig. 2 a-c - Ultrastructure of the ground-mass of the Marker-bed sampled at 20 cm from the core top in Core BAN-88 09 TW. Sample treated as for fig. 1. A few coccoliths (arrows) are present in the depressions. a) Micronodule embedded in a clay matrix; 1600x. b) and c) Abundant bacterial colonies; 4500x and 21000x respectively.

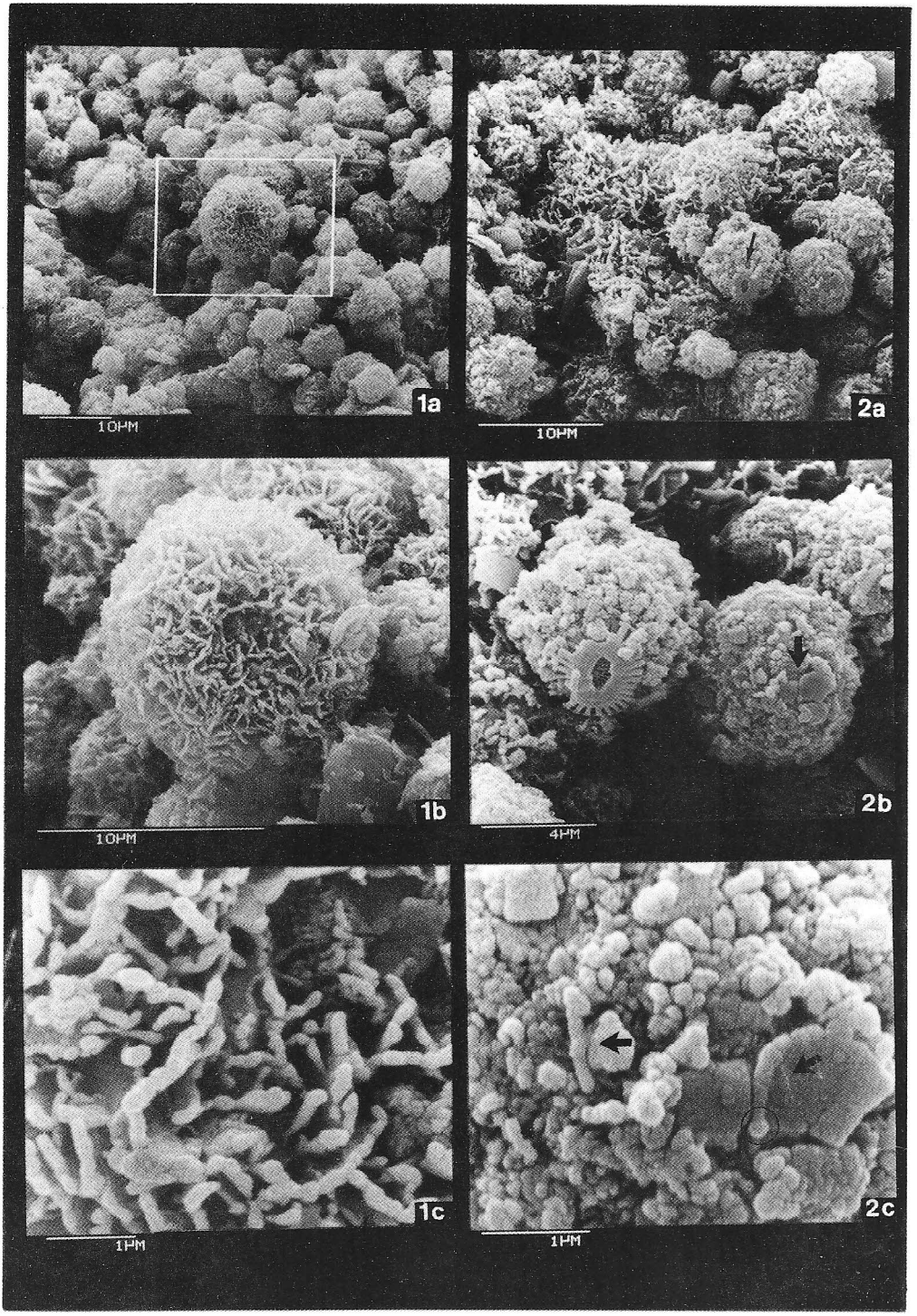
1a
10µm
2a
10µm
1b
10µm
2b
4µm
1c
1µm
2c
1µm

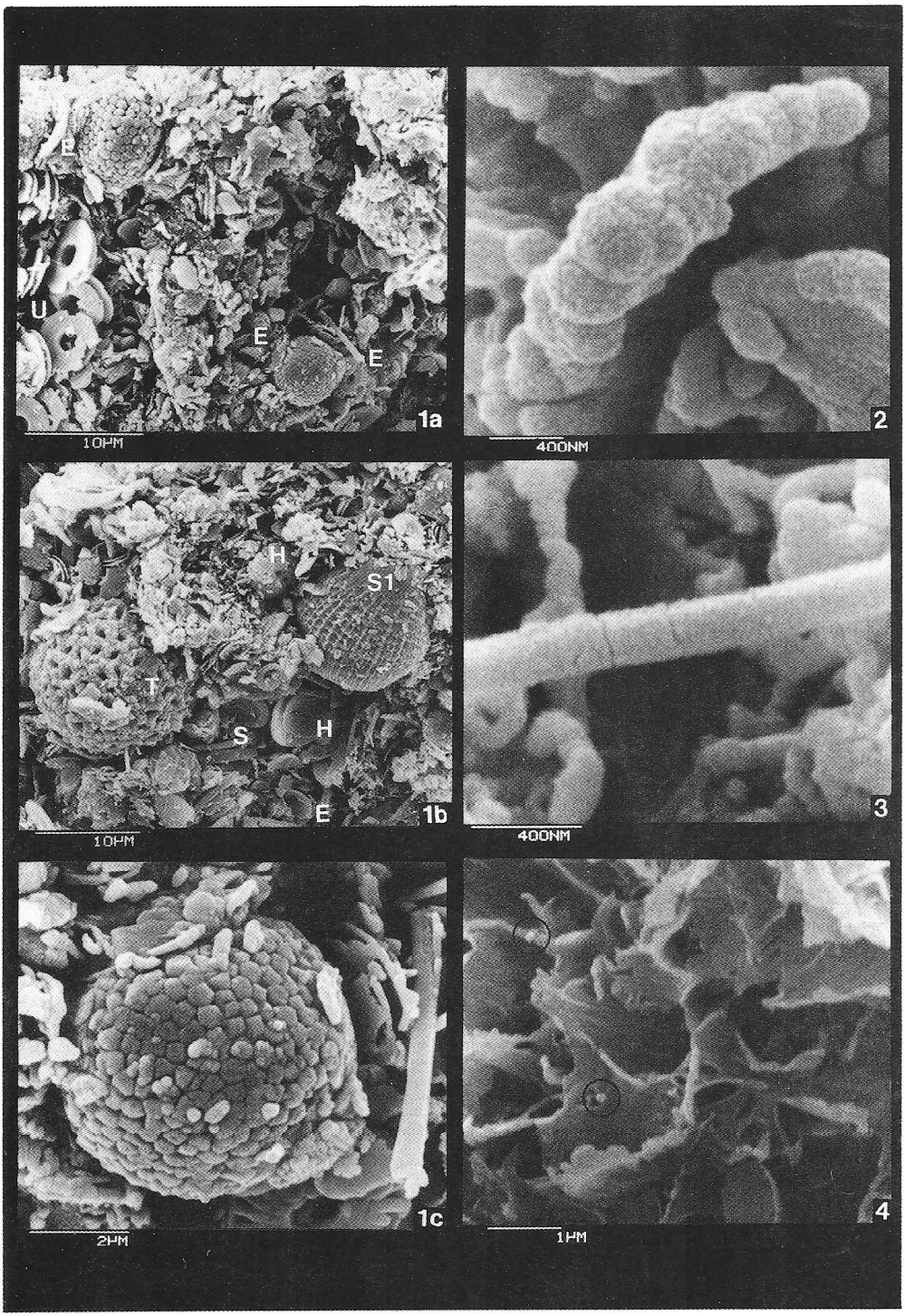
E
U
E
E
1a
10µM
400NM
2
H
S1
T
S
H
E
1b
10µM
400NM
3
1c
2µM
1µM
4

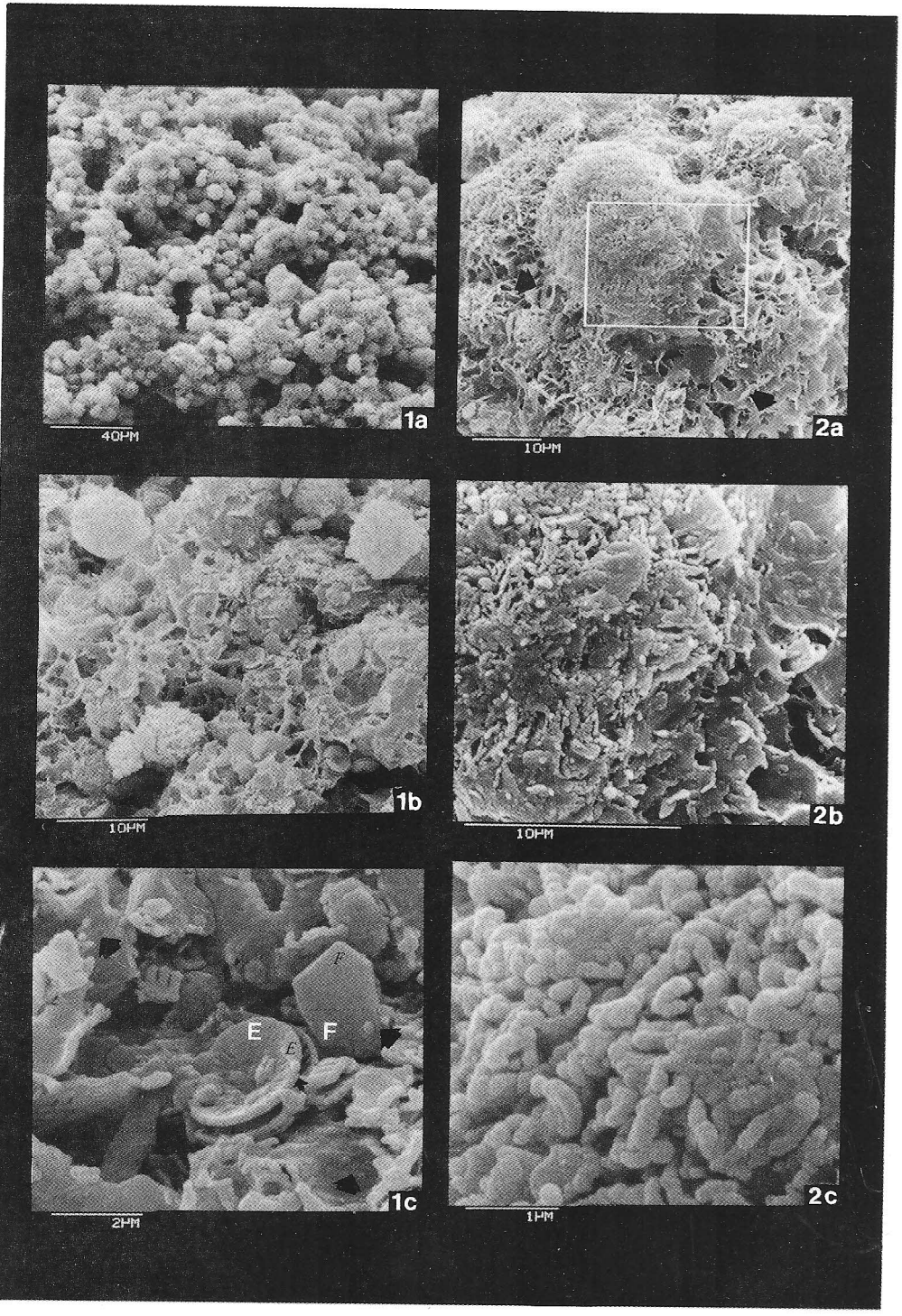
40µM
1a
10µM
2a
1b
10µM
10µM
2b
E
F
E
F
2µM
1c
1µM
2c

PUBBLICAZIONI DI CARATTERE GENERALE

Hemleben Ch., Spindler M., & Anderson O.R. (1989) - **Modern Planktonic Foraminifera.** Vol. di 337 pp., 109 fig., Springer-Verlag, DM 178, New York, Berlin, Heidelberg, London, Tokyo.

Scopo di questo volume è raccogliere tutti i dati relativi alle odierne conoscenze sulla biologia dei foraminiferi planctonici attuali, sulle tecniche di coltura in laboratorio e sulle metodologie di studio.

Il libro è suddiviso in 12 capitoli e contiene una documentazione fotografica estremamente esauriente.

I primi capitoli riguardano esclusivamente le classificazioni (vengono distinte forme spinose e non spinose) con descrizione delle specie più rappresentative, e le tecniche di raccolta in mare e colture in laboratorio. Le tecniche di coltura comprendono anche le analisi del comportamento di questi organismi al variare delle condizioni ambientali simulate in laboratorio (tipo e frequenza di alimentazione, intensità della luce ecc.).

I capitoli successivi invece trattano in modo dettagliato tutti gli aspetti della biologia dei foraminiferi planctonici messi anche a confronto con le forme bentoniche e, quando possibile, con organismi di diversa natura come i radiolari. Sono poi prese in esame sia l'ultrastruttura della cellula e i vari componenti di questa, che le principali attività biologiche, come attività trofica e nutrizione, crescita, costruzione del guscio, riproduzione. Particolare attenzione è stata dedicata alla riproduzione (che nei foraminiferi planctonici avviene per gametogenesi), alle strutture che modificano la morfologia dei gusci durante questo processo (ispessimenti gametogenetici), ed al loro significato.

Un capitolo è poi dedicato all'ecologia di questi organismi, alla dinamica delle popolazioni, alla loro distribuzione orizzontale, verticale, stagionale e all'influenza delle masse d'acqua su questi parametri.

Sedimentazione e dissoluzione dei gusci nelle acque marine sono gli argomenti trattati nell'ultima parte del volume, che si conclude con una schematica trattazione sulle tecniche di analisi degli isotopi stabili (Ossigeno e Carbonio) sui gusci e sull'interpretazione delle curve isotopiche per ricostruzioni paleoclimatiche e paleoambientali.

S. SPEZZAFERRI

Premoli Silva I., Coccioni R. & Montanari A. (Eds.) (1988) - **The Eocene/Oligocene boundary in the Marche-Umbria basin (Italy).** IUGS Commission on Stratigraphy. Vol. di 268 pp., Ancona.

Il volume consiste in una raccolta di studi interdisciplinari presentati al convegno sul limite Eocene/Oligocene tenutosi ad Ancona (Monte Conero) dal 1 al 3 Ottobre 1987. Durante questo convegno sono stati presi in esame gli aspetti biostratigrafici, litostratigrafici, sedimentologici, petrologici e geochimici della Sezione di Massignano (Scaglia Variegata/Scaglia Cinerea eocenica/oligocenica) a confronto con le altre successioni Umbro-Marchigiane. Scopo principale era la ricerca di una nuova sezione da proporre come Sezione tipo del limite Eocene/Oligocene, alla luce dei risultati emersi dal Progetto 174 IGCP.

La sezione di Massignano è stata studiata in dettaglio da ricercatori sia italiani che stranieri in laboratori diversi e le analisi, condotte spesso sugli stessi campioni, hanno dato risultati confrontabili. In base a questi è stata possibile una consistente reiterazione di precedenti successioni biostratigrafiche correlate alle corrispondenti successioni magnetostratigrafiche. È stata poi messa in evidenza l'importanza stratigrafica degli isotopi dello Stronzio, dell'Iridio e dei records degli isotopi stabili (soprattutto del Carbonio) che permettono correlazioni a livello mondiale indipendentemente dalla latitudine e dallo stato di conservazione dei fossili. Di fondamentale importanza sono state le datazioni dirette dei sedimenti, dei bioeventi e delle Zone magnetiche, sulla base delle analisi radioisotopiche delle biotiti di origine vulcanica in orizzonti intercalati nella sequenza pelagica della Scaglia Variegata/Scaglia Cinerea del Bacino Umbro-Marchigiano. Le età ottenute con questo tipo di analisi sulle biotiti della Sezione di Massignano, infine, suggeriscono che il limite Eocene/Oligocene è in realtà più giovane di 34.5 milioni di anni.

Come conclusione viene proposta la sezione di Massignano, come potenziale Sezione tipo del limite Eocene/Oligocene, il quale viene inoltre basato sull'evento biostratigrafico dell'estinzione delle Hantkenine.

S. SPEZZAFERRI